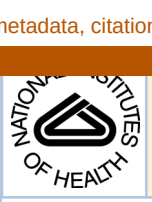

Published in final edited form as:
Circulation. 2011 February 15; 123(6): 621–630. doi:10.1161/CIRCULATIONAHA.110.970038.

Augmented Expression and Activity of Extracellular Matrix-Degrading Enzymes in Regions of Low Endothelial Shear Stress Colocalize With Coronary Atheromata With Thin Fibrous Caps in Pigs

Yiannis S. Chatzizisis, MD, PhD[*], **Aaron B. Baker, PhD**[*], **Galina K. Sukhova, PhD**[*], **Konstantinos C. Koskinas, MD, MSc**[*], **Michail I. Papafaklis, MD, PhD**, **Roy Beigel, MD**, **Michael Jonas, MD**, **Ahmet U. Coskun, PhD**, **Benjamin V. Stone**, **Charles Maynard, PhD**, **Guo-Ping Shi, ScD, PhD**, **Peter Libby, MD**, **Charles L. Feldman, ScD**, **Elazer R. Edelman, MD, PhD**, and **Peter H. Stone, MD**

Cardiovascular Division, Brigham and Women's Hospital, Harvard Medical School, Boston, MA (Y.S.C., G.K.S., K.C.K., M.I.P., G.-P.S., P.L., C.L.F., E.R.E., P.H.S.); Harvard–MIT Division of Health Sciences and Technology, Massachusetts Institute of Technology, Cambridge, MA (Y.S.C., A.B.B., K.C.K., R.B., M.J., B.V.S., E.R.E.); Mechanical and Industrial Engineering, Northeastern University, Boston, MA (A.U.C.); and Department of Health Services, University of Washington, Seattle (C.M.).

Abstract

Background—The molecular mechanisms that determine the localized formation of thin-capped atheromata in the coronary arteries remain unknown. This study tested the hypothesis that low endothelial shear stress augments the expression of matrix-degrading proteases and thereby promotes the formation of thin-capped atheromata.

Methods and Results—Intravascular ultrasound–based, geometrically correct 3-dimensional reconstruction of the coronary arteries of 12 swine was performed in vivo 23 weeks after initiation of diabetes mellitus and a hyperlipidemic diet. Local endothelial shear stress was calculated in plaque-free subsegments of interest (n=142) with computational fluid dynamics. At week 30, the coronary arteries (n=31) were harvested and the same subsegments were identified. The messenger RNA and protein expression and elastolytic activity of selected elastases and their endogenous inhibitors were assessed. Subsegments with low preceding endothelial shear stress at week 23 showed reduced endothelial coverage, enhanced lipid accumulation, and intense infiltration of activated inflammatory cells at week 30. These lesions showed increased expression of messenger RNAs encoding matrix metalloproteinase-2, -9, and -12, and cathepsins K and S relative to their endogenous inhibitors and increased elastolytic activity. Expression of these

Correspondence to Peter H. Stone, MD, Cardiovascular Division, Brigham and Women's Hospital, Harvard Medical School, 75 Francis St, Boston, MA 02115. pstone@partners.org.

[*]Drs Chatzizisis, Baker, Sukhova, and Koskinas contributed equally to this article.

Guest Editor for this article was Mark B. Taubman, MD.

The online-only Data Supplement is available with this article at http://circ.ahajournals.org/cgi/content/full/CIRCULATIONAHA.110.970038/DC1.

Disclosures
None.

enzymes correlated positively with the severity of internal elastic lamina fragmentation. Thin-capped atheromata developed in regions with lower preceding endothelial shear stress and had reduced endothelial coverage, intense lipid and inflammatory cell accumulation, enhanced messenger RNA expression and elastolytic activity of MMPs and cathepsins, and severe internal elastic lamina fragmentation.

Conclusions—Low endothelial shear stress induces endothelial discontinuity and accumulation of activated inflammatory cells, thereby augmenting the expression and activity of elastases in the intima and shifting the balance with their inhibitors toward matrix breakdown. Our results provide new insight into the mechanisms of regional formation of plaques with thin fibrous caps.

Keywords

atherosclerosis; shear stress; endothelium; inflammation; proteases

Despite the systemic nature of risk factors for atherosclerosis, lesion distribution is geometrically focal and heterogeneous. Multiple atherosclerotic lesions at different stages of progression commonly coexist in an individual artery.[1] Some atherosclerotic lesions with thin fibrous caps appear particularly prone to acute disruption and precipitation of an acute coronary syndrome.[2] These lesions often do not limit blood flow and therefore are not detected or specifically treated before they rupture.

Clinical Perspective on p 630

Histopathological studies in animal models of atherosclerosis have demonstrated that such atherosclerotic lesions with high-risk characteristics preferentially develop in regions of particularly low endothelial shear stress (ESS).[3–5] However, the molecular mechanisms and the triggering pathophysiological determinants responsible for the local formation of plaques with thin fibrous caps remain unknown. Prior in vitro and ex vivo experiments have indicated that low ESS can augment the expression and activity of matrix-degrading proteases such as matrix metalloproteinase (MMP)-2 and MMP-9[6] and cathepsins K and L.[7] These enzymes participate in the pathobiology of atherosclerosis in that they promote the degradation of the extracellular matrix macromolecules in the arterial wall and fibrous cap, facilitating the transmigration of inflammatory cells and vascular smooth muscle cells into the plaque.[8,9] However, most of these studies used cultured cells, which lack the complex environment of the atherosclerotic vascular wall in vivo. The in vivo role of low ESS in the expression and activity of matrix-degrading proteases and their subsequent involvement in the development of atheromata with thin fibrous cap remain unknown.

This study tested the hypothesis in vivo that low ESS augments messenger RNA (mRNA) expression and activity of elastolytic proteases in coronary atherosclerotic plaques relative to their endogenous inhibitors, thereby shifting the plaque to a more elastolytically active state and facilitating the progression and differentiation of that plaque to an atheroma with thin fibrous cap. We studied pigs with advanced atheromata similar to those observed in humans.[10]

Methods

Porcine Model of Atherosclerosis

A detailed description of the methods is presented in the online-only Data Supplement. Briefly, 12 male Yorkshire swine were rendered diabetic through streptozotocin injection and fed a high-fat diet.[3,10] Twenty-three weeks (baseline) after the induction of diabetes mellitus and initiation of the high-fat diet, the pigs underwent in vivo vascular profiling of all the major epicardial coronary arteries to assess the local ESS along the surface of the

reconstructed lumen, as previously described.[3,4,11,12] At week 30 (follow-up), the animals underwent repeat vascular profiling and were euthanized, and the coronary arteries were harvested and analyzed histopathologically.

In Vivo Vascular Profiling

ESS was calculated on the lumen surface of the reconstructed coronary arteries at baseline and correlated with the histopathology, mRNA and protein expression, and elastolytic activity of matrix-degrading enzymes at follow-up. We selected 142 arterial subsegments of interest 3 mm in length on the basis of different levels of baseline ESS magnitude.[3] The selected subsegments exhibited varied 3-dimensional geometry. We focused on subsegments free of apparent atherosclerosis by intravascular ultrasound at baseline (maximum intima-media thickness ≤0.5 mm by intravascular ultrasound) because this allowed us to study the role of ESS in the initiation and progression of coronary atherosclerosis through multiple natural history stages, culminating in severe plaques with features found in ruptured plaques in humans.

Baseline ESS was measured with computational fluid dynamics as previously described.[3,4,11] Local ESS was averaged in each 3-mm-long subsegment and classified as either low ESS (<1.00 Pa; n=79; mean, 0.67±0.03 Pa) or higher ESS (≥1.00 Pa; n=63; mean, 1.59±0.07 Pa). The arterial remodeling response to plaque formation was estimated at follow-up by intravascular ultrasound in each subsegment and classified as compensatory expansive, excessive expansive, or constrictive.[3,4]

Histopathological, mRNA, and In Situ Zymography Analyses

The subsegments were located in the harvested coronary arteries by identifying several major and readily visible side branches on the ESS and wall thickness maps, as well as on the harvested arteries.[3] The middle portion of the subsegments was cryosectioned at 7-μm thickness. Verhoeff elastin and Oil Red O staining, as well as CD31 and CD45 immunostaining, were performed in each cryosection for the assessment of intima-to-media ratio (IM), lipid accumulation, luminal endothelial cell coverage, and inflammatory cell infiltration, respectively. We performed immunostaining for the class II histocompatibility complex (MHC-II) molecules in serial sections with CD45 immunostaining to assess the plaque content of activated inflammatory cells.[13] For quantification of all histological assays, we measured the percent of the intima with positive staining.

mRNA was harvested from the intima and media of the subsegments. mRNA encoding selected matrix-degrading elastolytic proteases (ie, MMP-2, MMP-9, MMP-12, and cathepsins K, L, and S) and their inhibitors (ie, tissue inhibitor of MMP [TIMP]-1, TIMP-2, and cystatin C) were measured by real-time reverse-transcriptase polymerase chain reaction (Table I in the online-only Data Supplement).

The protein expression of MMP-2 and cathepsin-S was assessed by immunohistochemistry and immunofluorescent staining in representative subsegments. The MMP- and cathepsin-mediated elastolytic activity was assessed and quantified by in situ zymography (ISZ).[14,15]

Lesions at follow-up were classified histopathologically into 3 categories[2,3]: (1) minimal lesions, defined as lesions with IM <0.15; (2) intermediate lesions, defined as lesions with IM ≥0.15 without evidence of fibrous cap; and (3) thin-capped atheromata, defined as lesions with IM ≥0.15 with a thin (<65 μm) fibrous cap overlying a lipid core. The integrity of the internal elastic lamina (IEL) was assessed in Verhoeff elastin–stained sections and classified into 4 grades.[3,16] The integrity of the IEL was correlated with the ESS at baseline and with the subsequent elastase expression and activity at follow-up.

Statistical Analyses

All analyses were performed with SPSS 17.0 (SPSS Inc, Chicago, IL) and Stata 10.0 (StataCorp LP, College Station, TX). Continuous variables are summarized as mean±SEM and categorical variables as actual numbers and percentages. To correct for systematic error introduced by the clustering of arterial subsegments within animals, several statistical methods were used. First, to investigate the association of continuous dependent variables (eg, CD31-positive endothelial cells, expression of matrix-degrading enzymes, content of activated macrophages) with categorical independent variables (eg, baseline ESS), mixed-effects ANOVA with the animal as random effect was used. Although ESS is a continuous variable, these analyses were performed by dichotomizing ESS as a categorical variable. Second, for analyses with continuous dependent (eg, expression of matrix enzymes) and continuous independent variables (eg, histopathological characteristic, cholesterol levels), linear regression was used. Finally, when the dependent variable was categorical (eg, lesion category, IEL grade), either ordinary or ordered logistic regression was used. In linear regression and logistic regression analyses, the SEs of the regression coefficient were adjusted for clustering of arterial subsegments within animals with the Huber White sandwich estimator. In all analyses, there were no missing values, and *P* values were adjusted for multiple comparisons of data with either the Scheffé or modified Bonferroni method. Findings were considered statistically significant at the 0.05 level.

The authors had full access to and take full responsibility for the integrity of the data. All authors have read and agree to the manuscript as written.

Results

Reduced CD31-Positive Endothelial Cells in Low-ESS Subsegments

In subsegments with low baseline ESS, the percentage of luminal periphery with CD31-positive endothelial cells was significantly reduced compared with subsegments with higher baseline ESS (Figure 1A). Inflammation was negatively associated with the percent of luminal periphery with CD31-positive endothelial cells (r=0.65, linear regression coefficient ±SE, −0.017±0.005; n=29; P<0.001), supporting the crucial role of endothelial integrity in intimal inflammatory cell infiltration. Figure 1D through 1G shows CD31 immunofluorescence and CD45 immunostaining in representative lesions with low and higher baseline ESS, respectively.

Increased Expression and Activity of Elastolytic MMPs in Low-ESS Subsegments

Subsegments with low baseline ESS had significantly higher levels of mRNAs encoding MMP-2, -9, and -12, as well as their endogenous inhibitors TIMP-1 and -2, compared with subsegments with higher baseline ESS (Figure 2A). Despite the parallel increase in mRNA expression of both MMPs and their inhibitors in low-ESS subsegments, the ratio of MMP to TIMP was higher in low-ESS subsegments, indicating an increase in MMP over TIMP expression in low- versus higher-ESS subsegments.

To investigate the potential factors associated with the expression of the investigated proteases, we applied mixed-effects ANOVA using the mRNA expression of the enzymes as the dependent variable. The lowest baseline ESS and increased total cholesterol were both significant predictors of mRNA levels of the proteases (Table II in the online-only Data Supplement). These results indicate that both local ESS and the magnitude of hypercholesterolemia independently determine the expression of these enzymes.

To assess the protein expression of the investigated enzymes, we performed immunohistochemical staining for MMP-2 in selected subsegments of low versus higher

baseline ESS. We found higher MMP-2 staining in low-ESS subsegments (Figure 2B through 2D) versus higher-ESS subsegments (Figure 2E), confirming our mRNA results.

In addition to mRNA expression, we assessed the enzymatic activity of MMPs by ISZ optimized for MMPs. Bright green fluorescence released from the elastin substrate by MMP activity was more pronounced in low-ESS subsegments (Figure 2F) compared with higher-ESS subsegments (Figure 2H). Quantification of fluorescence intensity in the intima, as previously described,[15] showed significantly higher elastolysis in subsegments of low versus higher ESS (40.2±5.2% versus 7.8±1.4%; $P<0.001$). Attenuation of the zymographic activity in low-ESS subsegments by the addition of the metalloenzyme inhibitor EDTA (20 mmol/L) in serial sections indicates the involvement of such enzymes in signal generation (Figure 2G).

Double-immunofluorescent staining for CD45 and MMP-2 localized MMP-2 protein to CD45-positive cell infiltration in subsegments of low baseline ESS (Figure 2I through 2K). Of note, zymographic activity also colocalized with regions of CD45-positive areas in low-ESS subsegments (Figure 2L through 2N). These results affirm that the inflammatory cells constitute the major cellular sources of MMPs in regions of low ESS.

Increased Expression and Activity of Elastolytic Cathepsins in Low-ESS Subsegments

Similar to the observations of the elastolytic MMPs, subsegments with low baseline ESS had 1.5- to 2-fold greater levels of mRNA for cathepsins K and S, as well as their endogenous inhibitor cystatin C, than subsegments with higher ESS (Figure 3A). Furthermore, cathepsin-mediated elastolytic activity, assessed by ISZ optimized for cathepsins, was more pronounced in low-ESS subsegments and colocalized with CD45-positive inflammatory cells (Figure 3B through 3D). The zymographic activity, quantified as the percentage area of intimal fluorescence, was higher in subsegments of low versus higher ESS (32.4±2.8% versus 11.6±0.9%; $P<0.001$; Figure 3D and 3G). Cathepsin-mediated zymographic activity was abolished by the addition of 10 mmol/L E64D, a sulfhydryl protease inhibitor, indicating the relative contribution of such enzymes to the zymographic signal (Figure 3E).

Double-immunofluorescent staining for CD45 and cathepsin S further confirmed the increased expression of cathepsin S, as well as the localization of cathepsin S protein, in CD45-positive inflammatory cells in subsegments of low baseline ESS (Figure 3H through 3J) versus subsegments of higher baseline ESS (Figure 3K).

Enhanced Content of Activated Inflammatory Cells in Subsegments of Low ESS

To evaluate the levels of inflammation in low- versus higher-ESS subsegments, we performed immunostaining for CD45-positive inflammatory cells. To assess the content of activated inflammatory cells, we also stained for MHC-II antigen as an indicator of activated leukocytes in response to proinflammatory cytokines such as interferon-γ.[13] Although the percentage of intimal area infiltrated with inflammatory cells did not differ significantly (Figure 4A), lesions with low baseline ESS displayed a higher percentage of the intimal area positive for MCH-II staining (8.8±1.2% versus 3.1±0.5%; $P<0.001$; Figure 4B and D through G). The relative proportion of inflammatory cells that were activated (MHC-II positive) was significantly elevated in plaques that originated from low ESS (43±3.9% versus 20.3±3.8%; $P<0.001$; Figure 4C). These findings agree with the augmented expression and activity of matrix-degrading enzymes by activated inflammatory cells in low-ESS subsegments.

Association of IEL Fragmentation With Increased Expression and Activity of Elastolytic Proteases

Plaques with severe IEL fragmentation (ie, grades 2 and 3) developed in subsegments with lower baseline ESS and had higher levels of mRNAs encoding MMP-9 and cathepsin K and increased ratios of MMP to TIMP and cathepsin to cystatin C compared with lesions with no or minimal IEL fragmentation (ie, grades 0 and 1; Figure 5A through 5E). Consistent with these results, we found increased elastolytic activity of MMPs and cathepsins by ISZ in low-ESS plaques with severe IEL fragmentation versus higher-ESS plaques with intact IEL (Figure 5F and 5G). These results indicate the preponderance of active elastases relative to their inhibitors in lesions with low baseline ESS and enhanced subsequent IEL fragmentation.

Lesions with excessive expansive remodeling were associated with the lowest baseline ESS values[3] and displayed larger lumen, external elastic membrane, and plaque volumes at follow-up (Figure I in the online-only Data Supplement). We also found a strong positive association of IEL fragmentation with excessive expansive remodeling (P=0.005; Table III in the online-only Data Supplement). Taken together, these results indicate that low baseline ESS is closely associated with the severity of IEL fragmentation and excessive expansive remodeling, likely through the increased expression and activity of elastolytic enzymes.

Differential Expression of Matrix-Degrading Proteases in Lesions of Differing Morphologies

All lesions were histopathologically classified at follow-up (week 30) into 3 categories: minimal lesions (n=26, 18.3%), intermediate lesions (n=56, 39.4%), and atheromata with thin fibrous cap (n=60, 42.3%). As previously published, both thin-capped atheromata and intermediate lesions developed in subsegments with lower baseline ESS compared with minimal lesions (thin-capped atheromata, 0.91±0.07 Pa; intermediate, 0.98±0.06 Pa; minimal, 1.69±0.12 Pa; P<0.001).[3] Of note, 72% of atheromata with thin caps developed at week 30 in subsegments with low baseline ESS (<1.0 Pa) at week 23, whereas 28% of atheromata with thin cap originated from arterial regions with particularly low baseline ESS (<0.6 Pa; Figure II in the online-only Data Supplement).

Thin-capped atheromata displayed reduced percent of lumen with CD31-positive endothelial cells (Figure 1B) and significantly increased mRNA levels of MMP-2 and MMP-9, as well as cathepsins K and S, compared with both minimal and intermediate lesions (Figure 6). Although thin-capped atheromata had increased levels of mRNAs encoding the protease inhibitors TIMP-1, TIMP-2, and cystatin C, the MMP-to-TIMP and cathepsin-to-cystatin mRNA ratios increased significantly, indicating a net increase in the elastolytic potential in atheromata with thin caps (Figure 6).

Hemodynamic, Histomorphological, and Molecular Determinants of the Development of Atheromata With Thin Fibrous Cap

We focused on a subgroup of 52 similarly sized lesions of intermediate histomorphology (IM, 0.3 to 0.9; Figure III in the online-only Data Supplement). These lesions were either small atheromata with thin fibrous cap (n=20), presumed precursors of advanced thin-capped atheromata of the type associated with fatally disrupted human plaques, or atheromata without evidence of fibrous cap (n=32). With this analysis, we assessed the relationship between prior hemodynamic environment (week 23) and the subsequent histopathological characteristics and protease profile (week 30) of comparably sized, intermediate-stage lesions to investigate the mechanisms that promote the evolution of each plaque type and the differential impact of different ESS magnitudes on plaque characteristic adjusting for the effect of ESS on plaque size.

These 2 lesion types had similar size (IM, 0.56±0.04 versus 0.53±0.03; *P*=0.44) and developed in pigs with similar hypercholesterolemia (628±14 versus 619±13 mg/dL; *P*=0.62) and hyperglycemia (216±19 versus 220±15 mg/dL; *P*=0.88). The local ESS preceding the development of small atheromata with thin fibrous cap tended to be lower than that in atheromata without fibrous cap (0.75±0.07 versus 1.00±0.09 Pa; *P*=0.08). There were marked differences between small atheromata with thin cap and atheromata without fibrous cap in terms of luminal CD31-positive endothelial cells (37±6% versus 72±3%; *P*<0.001; Figure 1C), relative lipid content (70±6% versus 53±4%; *P*=0.02), and relative inflammatory cells content (43±8% versus 27±4%; *P*=0.06). With regard to the protease profile, small atheromata with thin cap had twice as much mRNA levels of MMP-2 and MMP-9, increased cathepsins K and S mRNAs, and a higher ratio of cathepsin to cystatin C compared with atheromata without fibrous cap (the Table). Small atheromata with thin cap were also associated with greater IEL fragmentation compared with atheromata without fibrous caps (*P*=0.05).

Discussion

This study explored in vivo the effect of local baseline ESS on the expression and elastolytic activity of selected proteases implicated in atherosclerosis and their endogenous inhibitors to investigate the mechanisms governing the local development of thin-capped atheromata. We induced a range of advanced lesions in the coronary arteries of diabetic, hyperlipidemic swine, including atheromata with thin fibrous caps resembling those found in humans.[3,10] In contrast to cell culture studies that examined protein expression under defined shear, we directly evaluated the plaque morphology and protease profile in regions of the coronary vasculature with defined in vivo assessment of local ESS. For the first time, we show that lesions in regions exposed to low ESS had reduced endothelial cell coverage, augmented infiltration of activated inflammatory cells, and substantially increased expression and enzymatic activity of elastases relative to their inhibitors. These enzymes likely contribute to fragmentation of elastin fibers in the IEL and promote excessive expansive remodeling response of the vessel wall, ultimately promoting the formation of atheromata with thin fibrous cap.

Role of Low ESS in the Expression and Activity of MMPs and Cathepsins

A complex combination of collagen, elastin, and proteoglycans makes up the extracellular matrix of the arterial wall and atheroma and determines the integrity of individual plaque. Prior cell culture studies have shown that low and oscillatory ESS augment the endothelial cell expression of MMPs that localize in atherosclerotic plaques.[8,17] In vivo studies in the carotid arteries of mice demonstrated further that low ESS increases the expression and activation of MMPs in atherosclerotic plaques.[5] These previous studies have not determined the relationship between low ESS and protease balance in the coronary arteries or in the intact animal. We now show that coronary arterial regions with low ESS develop lesions with greatly enhanced MMP-2, MMP-9, and MMP-12 expression and elastolytic activity. Although the exact role of MMP-9, particularly in plaque stability, rupture, and healing, is not yet conclusive,[18] our present results are in accordance with existing clinical and experimental data that strongly support the role of MMP-9 in plaque destabilization and rupture.[19]

ESS regulates gene expression through several mechanisms, including activation of shear stress response elements in promoters and increased levels of the transcription factors KLF-2 and KLF-4.[1] Subsequent production of proinflammatory cytokines and chemokines in the intima can in turn promote the accumulation and activation of inflammatory cells and augment protease release from their key cellular sources (ie, endothelial cells, macrophages, and vascular smooth muscle cells).[8] Low ESS can also directly stimulate MMP gene

expression in endothelial cells through activation of nuclear factor-κB.[17,20] TIMP gene expression also increases in atherosclerotic lesions exposed to low ESS, but our data indicate a net increase in proteolytic activity in these regions.

In addition to the MMPs, several other elastases, including cysteinyl cathepsins, participate in extracellular matrix breakdown in atheromata.[9] Cell culture studies have previously shown that low and oscillatory ESS augment the endothelial cell expression of cathepsins K and L.[7] The present study provides novel in vivo evidence that coronary artery subsegments exposed to low ESS have enhanced mRNA and protein expression, as well as elastolytic activity, of cathepsins. Subsequent stimulation of low-ESS–mediated cytokine- and nuclear factor-κB–dependent pathways similar to those for MMPs appears to promote the expression of cathepsins, shifting the local arterial vascular wall toward a more elastolytic state.[1]

Pathobiological Mechanisms Responsible for the Evolution of Atheromata With Thin Fibrous Cap

We have previously shown that low ESS influences the evolution of coronary plaques toward lesions with characteristics of high risk for rupture[4] and that the magnitude of low ESS associates with the development of late-stage thin-capped atheromata through enhancement of local inflammation. [3] Little is known, however, about the molecular events that determine the evolution of an early or intermediate lesion to a late-stage thin-capped atheroma. We addressed this question of molecular pathobiological determinants by analyzing a subgroup of 52 similarly sized lesions at an intermediate stage of development. Our analyses demonstrated that early plaques with thin fibrous caps and more intense inflammation developed in arterial regions with lower ESS compared with those plaques with no fibrous cap. Furthermore, the inflamed thin-capped atheromata had markedly increased mRNA expression and elastolytic activity of matrix-degrading enzymes compared with atheromata without fibrous cap. These results establish that the local hemodynamic stimulus of low ESS closely associates with the expression of elastolytic proteases during the early and intermediate stages of atherosclerosis. At the molecular level, low ESS favors endothelial dysfunction and subsequent attenuation in the expression of the cassette of “atheroprotective” genes,[1,21] influx and activation of inflammatory cells into the intima, production of extracellular matrix-degrading enzymes (including gelatinases and elastases), and intimal extracellular matrix dissolution. Products of intimal inflammatory cells can stimulate vascular smooth muscle cells to migrate from the media to the intima through IEL fenestrae[22] and foster plaque growth and formation of the fibrous cap, which overlies the lipid core, yielding an early atheroma with fibrous cap. Through the IEL discontinuity, which has also been described in human coronary plaques,[23] the inflammatory cells can also extend to the media where they elaborate matrix-degrading enzymes and promote expansive remodeling of the vascular wall. In such a locally expanded vascular region, the local ESS becomes even lower, as previously demonstrated,[3,4] and initiates a self-perpetuating vicious cycle of low ESS, endothelial dysfunction, inflammation, matrix-degrading activity, and wall expansion.[3,4] The intense matrix degradation may progressively drive the evolution of an early small atheroma to a high-risk thin-capped atheroma.

Although a majority (72%) of thin-capped atheromata developed in subsegments of low ESS, 28% of thin-capped atheromata originated from regions with higher baseline ESS. Furthermore, although the mRNA expression and activity of the matrix-degrading proteases were augmented in regions of low ESS, we found some heterogeneity in the expression of these enzymes even in regions of similarly low ESS. Taken together, our results suggest that low ESS clearly promotes high-risk plaque progression and augments the expression of the elastolytic proteases, but other local or systemic factors that were not analyzed in the present study such as the severity of hypercholesterolemia, vascular remodeling, and wall structural characteristics may also be in play.[24]

High ESS may induce pathobiological responses within the plaque that exacerbate plaque fragility, as suggested by the association of high ESS with high strain, a possible marker of vulnerable plaque composition.[25] Furthermore, human studies have shown that localized high shear stress may constitute a trigger for fibrous cap rupture.[26] The nature and specific magnitude of ESS responsible for plaque rupture remain to be elucidated.

Study Limitations

The arterial subsegments we investigated were not randomly selected; instead, they were identified a priori on the basis of ESS distribution. We were careful to include subsegments across a spectrum of baseline ESS magnitudes but could still have introduced selection bias in our samples, especially because we were dealing with a restricted number of animals. Like all studies, use of a larger number of animals at multiple times would have been beneficial if feasible. The power of the study increased, however, by investigating multiple sub-segments in each coronary artery (average, 5 subsegments per artery).

The fibrous cap thickness was measured in Oil Red O–stained sections. Although this is the standard method for assessing fibrous cap thickness in human arterial sections, it does not provide simultaneous staining of both the fibrous and lipid components of the plaque. In our analyses, we assumed that prominent staining for lipids with Oil Red O dye correlated with a loss of fibrous components in this region of the arterial section. A detailed description of the limitations of computational fluid dynamics and histopathological analyses is provided in the online-only Data Supplement.

Conclusions

Low ESS induces endothelial discontinuity and accumulation of activated inflammatory cells, thereby augmenting the expression and elastolytic activity of extracellular matrix-degrading proteases in the intima and shifting the balance with their inhibitors toward matrix breakdown. These mechanisms may contribute critically to extracellular matrix remodeling during the formation and evolution toward high-risk, rupture-prone coronary atherosclerotic plaque.

Supplementary Material

Refer to Web version on PubMed Central for supplementary material.

Acknowledgments

We acknowledge the contribution of Dr Ross Gerrity, who passed away during the completion of this work. We gratefully acknowledge Michelle Lucier, Gail MacCallum, and Eugenia Shvartz for their invaluable technical assistance.

Sources of Funding

This work was supported by grants from Novartis Pharmaceuticals Inc and Boston Scientific Inc (to Drs Stone and Feldman); the George D. Behrakis Research Fellowship (to Drs Chatzizisis, Koskinas, and Papafaklis); the Hellenic Heart Foundation (to Drs Chatzizisis and Papafaklis); the Hellenic Atherosclerosis Society (to Dr Chatzizisis); the Alexander Onassis Public Benefit Foundation (to Dr Chatzizisis); the Propondis Foundation (to Dr Chatzizisis); the Hellenic Harvard Foundation (to Drs Chatzizisis and Papafaklis); the A.G. Leventis Foundation (to Dr Chatzizisis); and the Philip Morris External Research Program (to Dr Baker), and a Scientist Development Grant from the American Heart Association (to Dr Baker). These studies were also supported in part by grant NIHR01 GM49039 (to Dr Edelman) and grant NHLBI HL80472 (to Dr Libby).

References

1. Chatzizisis YS, Coskun AU, Jonas M, Edelman ER, Feldman CL, Stone PH. Role of endothelial shear stress in the natural history of coronary atherosclerosis and vascular remodeling: molecular, cellular and vascular behavior. J Am Coll Cardiol. 2007; 49:2379–2393. [PubMed: 17599600]
2. Virmani R, Kolodgie FD, Burke AP, Farb A, Schwartz SM. Lessons from sudden coronary death: a comprehensive morphological classification scheme for atherosclerotic lesions. Arterioscler Thromb Vasc Biol. 2000; 20:1262–1275. [PubMed: 10807742]
3. Chatzizisis YS, Jonas M, Coskun AU, Beigel R, Stone BV, Maynard C, Gerrity R, Daley W, Campbell R, Elazer ER, Feldman CL, Stone PH. Prediction of the localization of high-risk coronary atherosclerotic plaques on the basis of low endothelial shear stress: an intravascular ultrasound and histopathology natural history study. Circulation. 2008; 117:993–1002. [PubMed: 18250270]
4. Koskinas KC, Feldman CL, Chatzizisis YS, Coskun AU, Jonas M, Maynard C, Baker AB, Edelman ER, Stone PH. Natural history of experimental coronary atherosclerosis and vascular remodeling in relation to endothelial shear stress: a serial, in vivo intravascular ultrasound study. Circulation. 2010; 121:2092–2101. [PubMed: 20439786]
5. Cheng C, Tempel D, van Haperen R, van der Baan A, Grosveld F, Daemen MJ, Krams R, de Crom R. Atherosclerotic lesion size and vulnerability are determined by patterns of fluid shear stress. Circulation. 2006; 113:2744–2753. [PubMed: 16754802]
6. Gambillara V, Montorzi G, Haziza-Pigeon C, Stergiopulos N, Silacci P. Arterial wall response to ex vivo exposure to oscillatory shear stress. J Vasc Res. 2005; 42:535–544. [PubMed: 16179795]
7. Platt MO, Ankeny RF, Shi GP, Weiss D, Vega JD, Taylor WR, Jo H. Expression of cathepsin K is regulated by shear stress in cultured endothelial cells and is increased in endothelium in human atherosclerosis. Am J Physiol Heart Circ Physiol. 2007; 292:H1479–H1486. [PubMed: 17098827]
8. Libby P. The molecular mechanisms of the thrombotic complications of atherosclerosis. J Intern Med. 2008; 263:517–527. [PubMed: 18410595]
9. Dollery CM, Libby P. Atherosclerosis and proteinase activation. Cardiovasc Res. 2006; 69:625–635. [PubMed: 16376322]
10. Gerrity RG, Natarajan R, Nadler JL, Kimsey T. Diabetes-induced accelerated atherosclerosis in swine. Diabetes. 2001; 50:1654–1665. [PubMed: 11423488]
11. Stone PH, Coskun AU, Kinlay S, Clark ME, Sonka M, Wahle A, Ilegbusi OJ, Yeghiazarians Y, Popma JJ, Orav J, Kuntz RE, Feldman CL. Effect of endothelial shear stress on the progression of coronary artery disease, vascular remodeling, and in-stent restenosis in humans: in vivo 6-month follow-up study. Circulation. 2003; 108:438–444. [PubMed: 12860915]
12. Chatzizisis YS, Giannoglou GD, Matakos A. In-vivo accuracy of geometrically correct three-dimensional reconstruction of human coronary arteries: is it influenced by certain parameters? Coron Artery Dis. 2006; 17:545–551. [PubMed: 16905967]
13. Schulte S, Sukhova GK, Libby P. Genetically programmed biases in Th1 and Th2 immune responses modulate atherogenesis. Am J Pathol. 2008; 172:1500–1508. [PubMed: 18467709]
14. Sun J, Sukhova GK, Wolters PJ, Yang M, Kitamoto S, Libby P, MacFarlane LA, Mallen-St Clair J, Shi GP. Mast cells promote atherosclerosis by releasing proinflammatory cytokines. Nat Med. 2007; 13:719–724. [PubMed: 17546038]
15. Schulte S, Sun J, Libby P, MacFarlane L, Sun C, Lopez-Ilasaca M, Guo-Ping Shi, Sukhova GK. Cystatin C deficiency promotes inflammation in angiotensin II-induced abdominal aortic aneurisms in atherosclerotic mice. Am J Pathol. 2010; 177:456–463. [PubMed: 20472891]
16. Sukhova GK, Wang B, Libby P, Pan JH, Zhang Y, Grubb A, Fang K, Chapman HA, Shi GP. Cystatin C deficiency increases elastic lamina degradation and aortic dilatation in apolipoprotein E-null mice. Circ Res. 2005; 96:368–375. [PubMed: 15653570]
17. Sun HW, Li CJ, Chen HQ, Lin HL, Lv HX, Zhang Y, Zhang M. Involvement of integrins, MAPK, and NF-kappaB in regulation of the shear stress-induced MMP-9 expression in endothelial cells. Biochem Biophys Res Commun. 2007; 353:152–158. [PubMed: 17174275]
18. Johnson JL, George SJ, Newby AC, Jackson CL. Divergent effects of matrix metalloproteinases 3, 7, 9, and 12 on atherosclerotic plaque stability in mouse brachiocephalic arteries. Proc Natl Acad Sci U S A. 2005; 102:15575–15580. [PubMed: 16221765]

19. Brunner S, Kim JO, Methe H. Relation of matrix metalloproteinase-9/ tissue inhibitor of metalloproteinase-1 ratio in peripheral circulating CD14+ monocytes to progression of coronary artery disease. Am J Cardiol. 2010; 105:429–434. [PubMed: 20152234]

20. Hajra L, Evans AI, Chen M, Hyduk SJ, Collins T, Cybulsky MI. The NF-kappa B signal transduction pathway in aortic endothelial cells is primed for activation in regions predisposed to atherosclerotic lesion formation. Proc Natl Acad Sci U S A. 2000; 97:9052–9057. [PubMed: 10922059]

21. Dai G, Vaughn S, Zhang Y, Wang ET, Garcia-Cardena G, Gimbrone MA Jr. Biomechanical forces in atherosclerosis-resistant vascular regions regulate endothelial redox balance via phosphoinositol 3-kinase/Akt-dependent activation of Nrf2. Circ Res. 2007; 101:723–733. [PubMed: 17673673]

22. Bentzon JF, Sondergaard CS, Kassem M, Falk E. Smooth muscle cells healing atherosclerotic plaque disruptions are of local, not blood, origin in apolipoprotein E knockout mice. Circulation. 2007; 116:2053–2061. [PubMed: 17938286]

23. Sukhova GK, Shi GP, Simon DI, Chapman HA, Libby P. Expression of the elastolytic cathepsins S and K in human atheroma and regulation of their production in smooth muscle cells. J Clin Invest. 1998; 102:576–583. [PubMed: 9691094]

24. Chatzizisis YS, Giannoglou GD. Coronary hemodynamics and atherosclerotic wall stiffness: a vicious cycle. Med Hypotheses. 2007; 69:349–355. [PubMed: 17343988]

25. Gijsen FJ, Wentzel JJ, Thury A, Mastik F, Schaar JA, Schuurbiers JC, Slager CJ, van der Giessen WJ, de Feyter PJ, van der Steen AF, Serruys PW. Strain distribution over plaques in human coronary arteries relates to shear stress. Am J Physiol Heart Circ Physiol. 2008; 295:H1608–H1614. [PubMed: 18621851]

26. Fukumoto Y, Hiro T, Fujii T, Hashimoto G, Fujimara T, Yamada J, Okamura T, Matsuzaki M. Localized elevation of shear stress is related to coronary plaque rupture: a 3-dimensional intravascular ultrasound study with in-vivo color mapping of shear stress distribution. J Am Coll Cardiol. 2008; 51:645–650. [PubMed: 18261684]

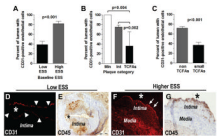

Figure 1.

Percentage of luminal periphery with CD-31–positive endothelial cells in (A) low-ESS (n=18) vs higher-ESS (n=11) subsegments, (B) minimal lesions (Min) vs intermediate lesions (Int) vs atheromata with thin fibrous cap (TCFAs), and (C) small atheromata with thin fibrous cap (small TCFAs) vs similar-sized atheromata without fibrous caps (nonTCFAs). Representative (D) CD31 immunofluorescence and (E) CD45 immunostaining in a lesion with low baseline ESS show endothelial discontinuity (arrowheads) and intense inflammatory cell accumulation respectively. Representative (F) CD31 immunofluorescence and (G) CD45 immunostaining in a lesion of higher baseline ESS show intact endothelium (arrows) and limited accumulation of inflammatory cells respectively. Asterisks indicate the lumen.

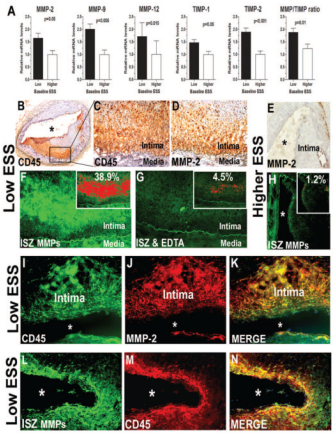

Figure 2.

Increased expression and activity of MMPs in low-ESS (n=79) vs higher-ESS (n=63) subsegments. A, Relative mRNA levels of MMP-2, MMP-9, MMP-12, TIMP-1, and TIMP-2 and the ratio of MMPs to TIMPs in low- vs higher-ESS subsegments. B, Representative immunostaining for CD45 in a low-ESS lesion. Higher magnification of (C) CD45 staining and (D) MMP-2 staining in the area selected by the black box in B. F, ISZ optimized for MMPs shows intense green fluorescence, indicating high elastolytic activity in serial sections with C and D. G, The MMP-inhibitor EDTA abolished elastolytic activity in the adjacent section. E, Absence of MMP-2 staining in a representative lesion of higher baseline ESS. H, Absence of MMP-mediated elastolytic activity in the same lesion as in E. Elastolytic activity–dependent fluorescence is shown in red in the insets in F through H. The percentage of intimal area with fluorescence intensity is indicated in each inset. I, Double immunofluorescence for (I) CD45 and (J) MMP-2 in a representative lesion of low ESS. K, Orange indicates colocalization of both antigens. L, Elastolytic activity (ISZ optimized for MMP) colocalizes with inflammatory cells infiltration (M, CD45 immunofluorescence applied in an adjacent section) in a lesion of low baseline ESS. N, Orange indicates colocalization. Asterisks indicate the lumen.

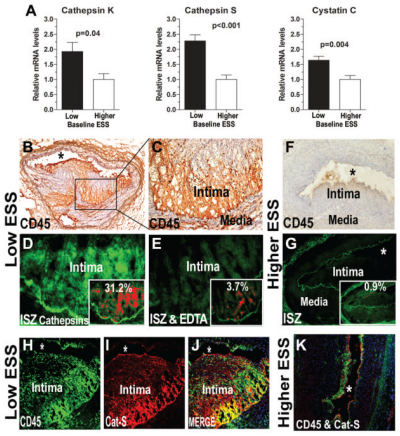

Figure 3.

Increased expression and activity of cathepsins in low-ESS (n=79) vs higher-ESS (n=63) subsegments. A, Relative mRNA levels of cathepsins K and S and cystatin C in low- vs higher-ESS sub-segments. B, Representative immunostaining for CD45 in a lesion of low baseline ESS. C, Higher magnification of the region selected by the black box in B. D, ISZ optimized for cathepsins shows intense green fluorescence, indicating high elastolytic activity, in the inflammatory cell–rich area. E, Addition of cathepsin inhibitor E64D eliminates the enzyme activity in the serial section. F, CD45 immunostaining and (G) ISZ in a representative lesion of higher baseline ESS. Elastolytic activity–dependent fluorescence is shown in red in the insets in D, E, and G. The percentage of intimal area with fluorescence intensity is indicated in each inset. Immunofluorescent staining for (H) CD45 and (I) cathepsin S in a representative lesion of low ESS shows the marked expression and colocalization of both antigens, indicated by the merge of H and I (J). K, Double-immunofluorescent staining for CD45 (green) and cathepsin S (red) in a subsegment of higher ESS. Asterisks denote the lumen.

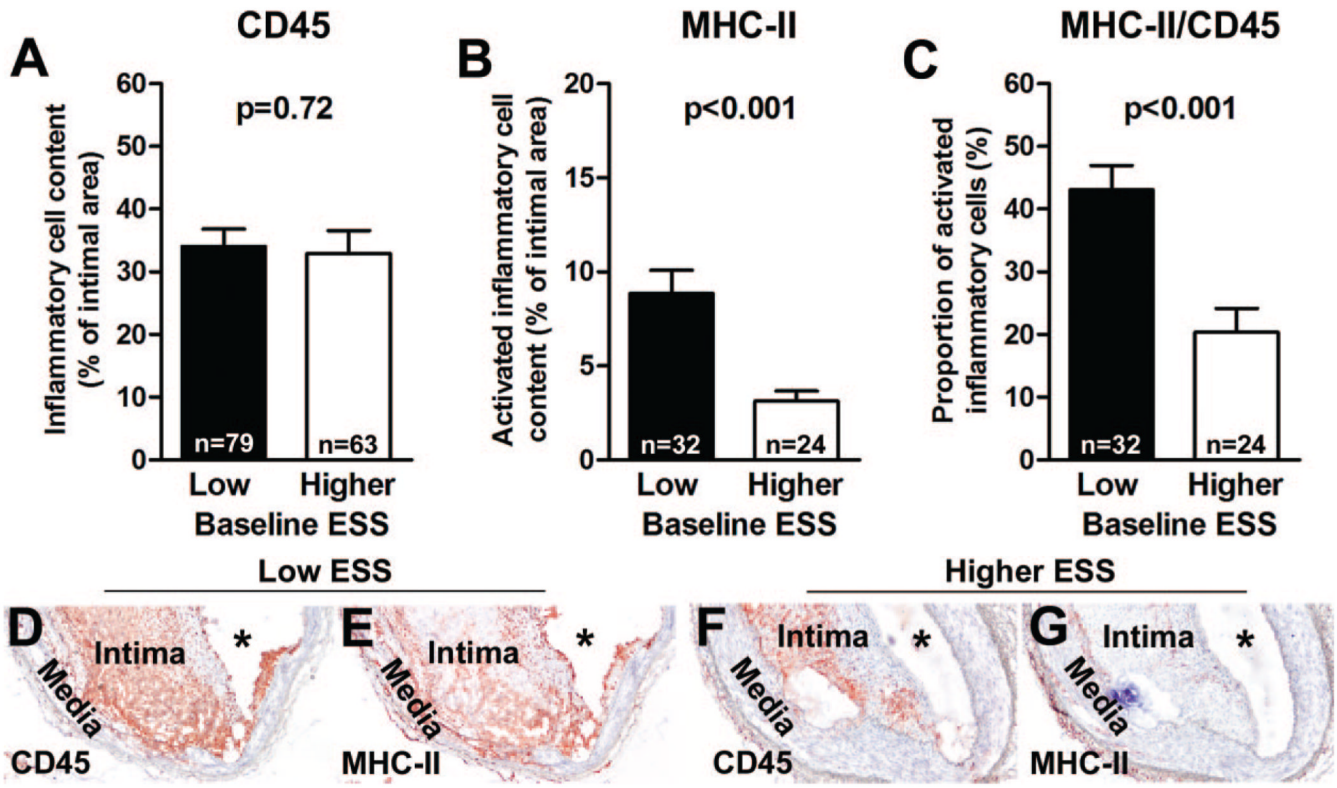

Figure 4.

Low-ESS subsegments contain more activated inflammatory cells compared with higher ESS subsegments. A, The percentage of CD45-positive intimal area did not differ between low-ESS (n=79) and higher-ESS (n=63) subsegments. However, low-ESS sub-segments (n=32) had (B) a higher percentage of MCH-II–positive intima area and (C) a higher proportion of activated (MHC-II–positive) inflammatory cells compared with higher-ESS subsegments (n=24). Microphotographs represent (D) CD45 staining and (E) MCH-II staining in parallel sections of a low-ESS subsegment and a higher-ESS subsegment (F and G, respectively). Asterisks indicate the lumen.

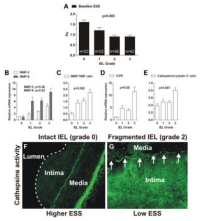

Figure 5.

The severity of IEL fragmentation correlates negatively with ESS levels and positively with MMP and cathepsin mRNA expression and activity. Association of each grade of IEL fragmentation with (A) baseline ESS, (B) relative mRNA expression of MMP-2 and MMP-9, (C) MMP/TIMP mRNA ratio, (D) relative mRNA expression of cathepsin K, and (E) cathepsins/cystatin C mRNA ratio. *P* values represent the overall association. In A through E, n=22 for IEL grade 1, n=22 for IEL grade 2, n=56 for IEL grade 3, and n=42 for IEL grade 4. Representative ISZ optimized for cathepsins in (F) a lesion of higher baseline ESS with intact IEL and (G) a lesion of low baseline ESS with moderate to severe IEL fragmentation; arrows depict the IEL breaks that colocalize with an increased elastolytic activity (bright green fluorescence) of cathepsins.

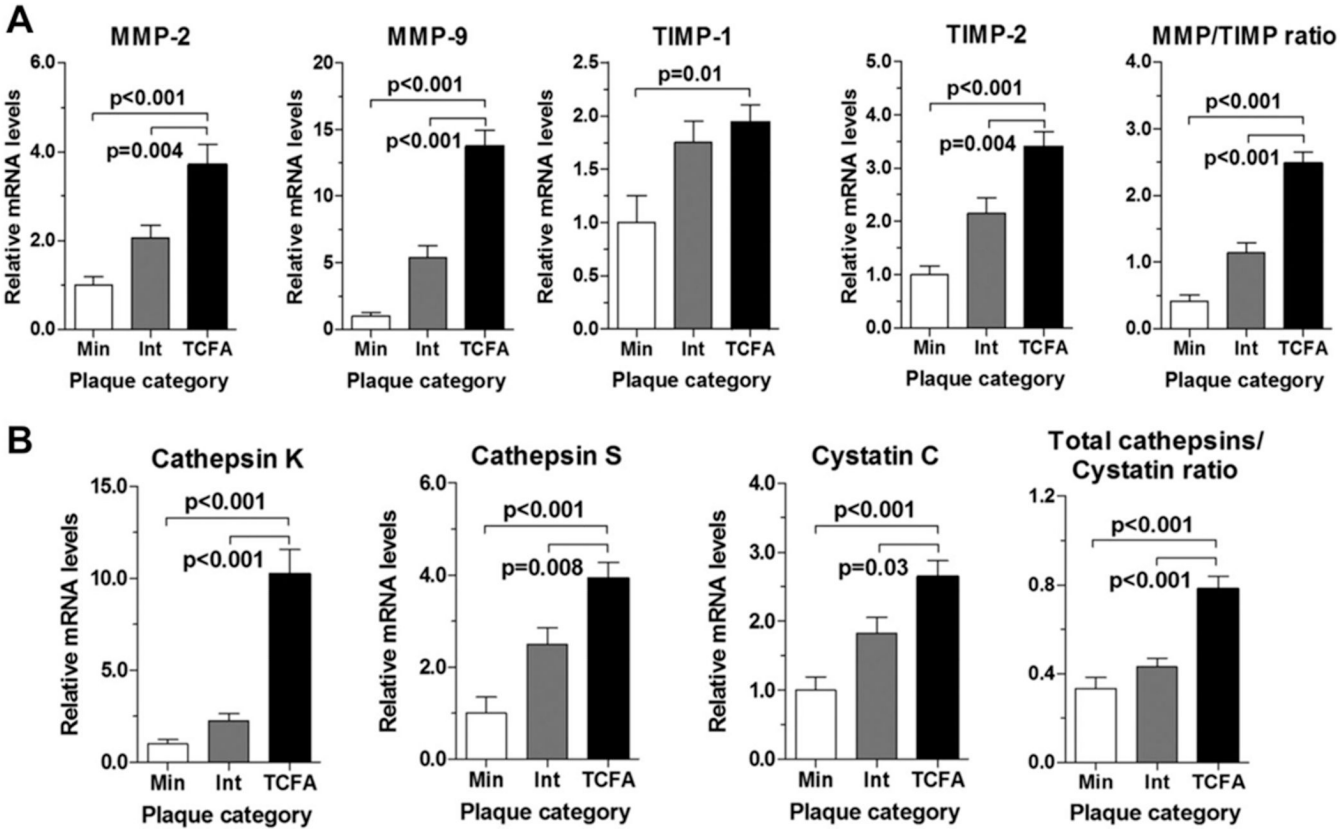

Figure 6.

Relative mRNA levels of MMPs, cysteine proteases, and their inhibitors in minimal lesions (Min), intermediate lesions (Int), and atheromata with thin fibrous cap (TCFA). A, The mRNA levels of MMP-2, MMP-9, TIMP-1, and TIMP-2 and the total MMP/TIMP ratio. B, The mRNA levels of cathepsin K, cathepsin S, and cystatin C and the cathepsins/cystatin C ratio.

Table

mRNA Expression of Matrix-Degrading Enzymes and Their Inhibitors in Atheromata Without Fibrous Cap Versus Small Thin-Capped Atheromata

	Plaque Category		
mRNA	**Atheromata Without Fibrous Cap (n=32)**	**Small Thin-Capped Atheromata (n=20)**	***P***
MMP-2	0.028±0.005	0.045±0.008	0.004
MMP-9	0.781±0.164	1.589±0.206	0.004
MMP-12	0.746±0.283	0.557±1.822	0.70
TIMP-1	0.282±0.036	0.365±0.059	0.41
TIMP-2	0.293±0.053	0.492±0.067	0.10
MMP/TIMP	1.429±0.202	2.604±0.343	0.07
Cathepsin K	0.156±0.027	0.500±0.093	0.005
Cathepsin L	0.064±0.010	0.075±0.013	0.20
Cathepsin S	0.363±0.067	0.682±0.093	0.023
Cystatin C	1.729±0.256	2.299±0.381	0.18
Total cathepsins/cystatin C	0.413±0.044	0.748±0.117	0.009

Values represent mean±SEM.